**Supporting Information**

# Constructing a novel three-dimensional scaffold with mesoporous $TiO_2$ nanotubes for potential bone tissue engineering

Yizao Wan [a,b], Peng Chang [a], Zhiwei Yang [a], Guangyao Xiong *[b], Ping Liu [a], Honglin Luo *[a]

[a] *School of Materials Science and Engineering, Tianjin University, Tianjin Key Laboratory of Composite and Functional Materials, Tianjin 300072, China*

[b] *School of Mechanical and Electrical Engineering, East China Jiaotong University, Nanchang 330013, China*

Authors for correspondence:

Prof. Guangyao Xiong, xiongguangyao@163.com

Dr. Honglin Luo, hlluotju@126.com

**Table S1** Pore structure parameters of $TiO_2$ nanotube scaffold.

| Samples | BET surface area ($m^2$ $g^{-1}$) | Pore volume ($cm^3$ $g^{-1}$) | Mesopore size (nm) |
|---|---|---|---|
| BC aerogel | 149.9 | 0.8954 | 13.73 |
| $TiO_2$/BC aerogel | 82.5 | 0.1180 | 3.50 |
| $TiO_2$ nanotube scaffold | 1629.0 | 2.565 | 3.30 |

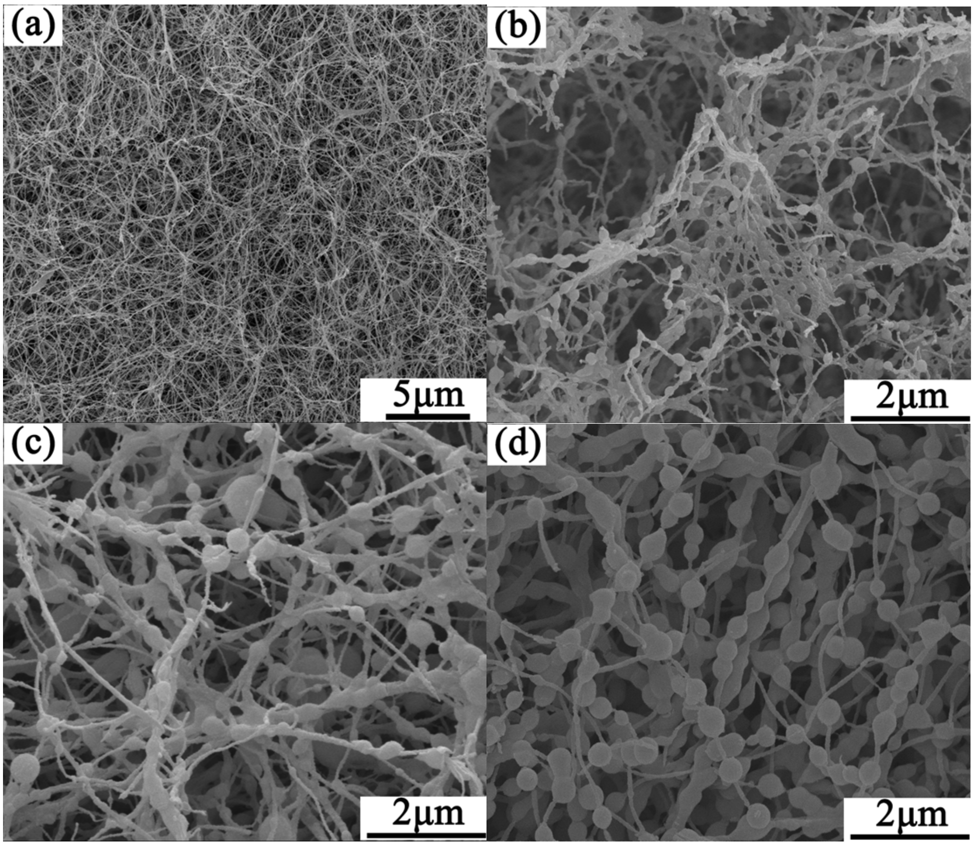


**Fig. S1** SEM images of pristine BC (a) and BC/$TiO_2$ hybrids synthesized in ethanol with different $Ti(OBu)_4$ concentrations ((b) 0.1 M, (c) 0.5, (d) 1.0 M).

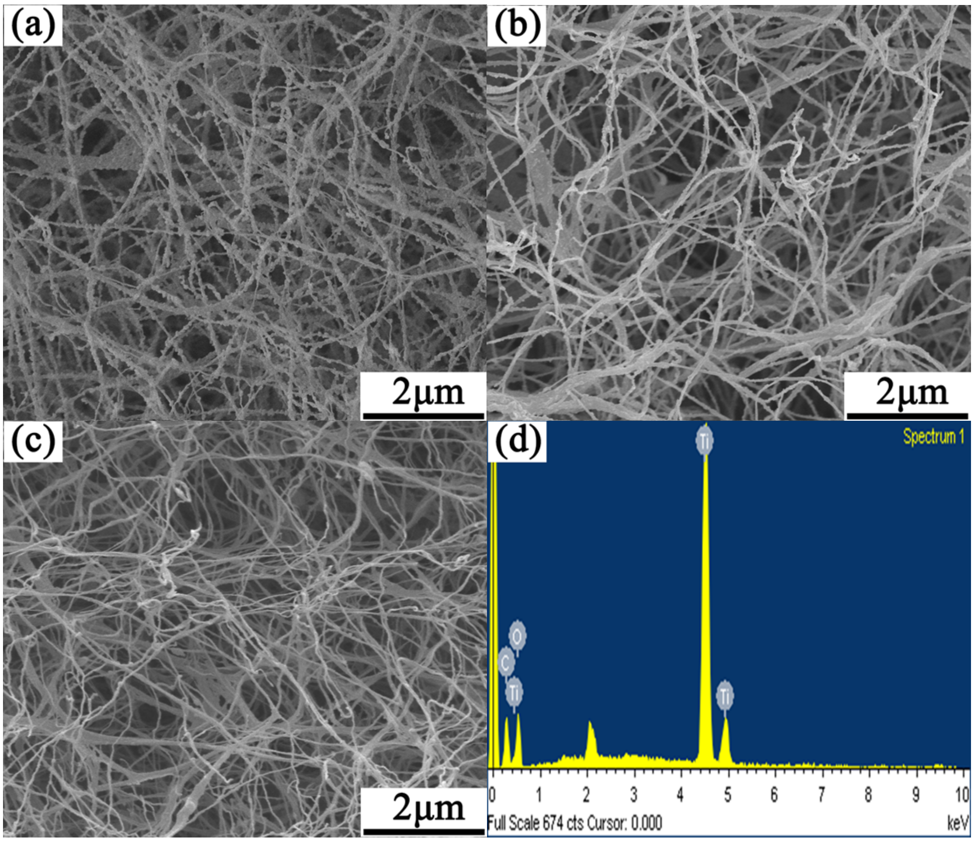


**Fig. S2** SEM images of BC/$TiO_2$ hybrids synthesized in isopropanol with different $Ti(OBu)_4$ concentrations ((a) 0.1 M, (b) 0.5 M, (c) 1.0 M) and EDS spectrum from the sample synthesized at 1.0 M (d).

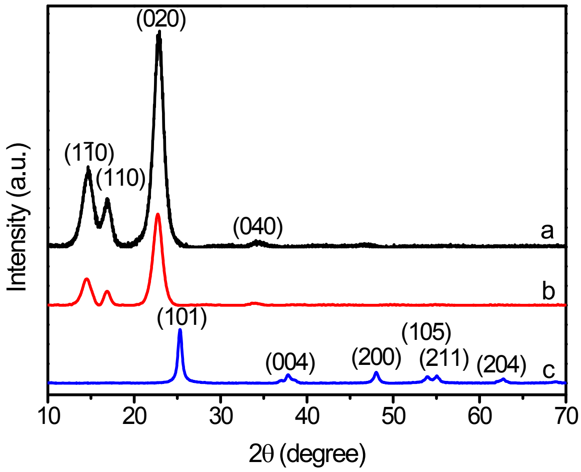


**Fig. S3** XRD patterns of BC (a), $TiO_2$/BC hybrid (b), and $TiO_2$ nanotubes calcined at 600 °C (c).

BC shows three main peaks at around 14.6, 16.9, and 22.9 °, corresponding to the crystalline planes of $(1\bar{1}0)$, (110), and (020) planes of cellulose type I.[2, 3] The intensity of these peaks in the spectrum of $TiO_2$/BC hybrid is much lower due to the presence of $TiO_2$ coating. The absence of the diffraction peaks of $TiO_2$ indicates the amorphous nature of the $TiO_2$ on BC nanofibers. In the spectrum of $TiO_2$ nanotubes calcined at 600 °C for 6 h, the transformation from amorphous to crystalline $TiO_2$ is demonstrated through the detection of the six characteristic peaks assigned to diffraction planes of (101), (004), (200), (105), (211), and (204) of anatase $TiO_2$ (JCPDS 21-1272). This is understandable since titania obtained through sol-gel hydrolysis is amorphous and crystallization can be induced by heat treatment.[4]

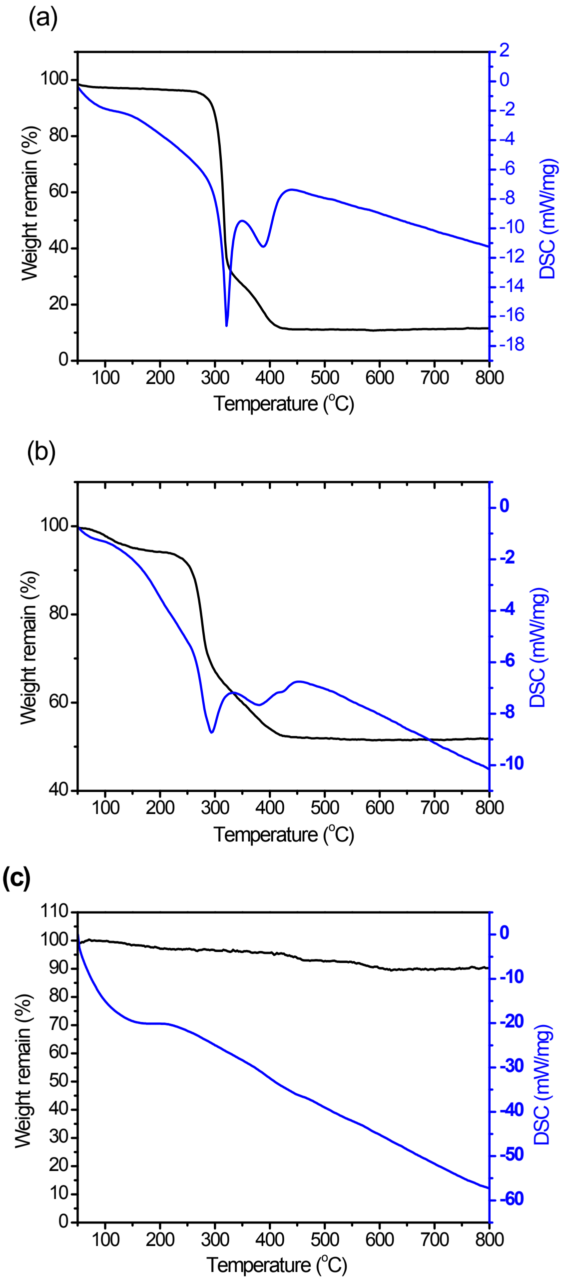


**Fig. S4** TGA-DSC curves of BC (a), BC/$TiO_2$ (b), and $TiO_2$ nanotubes (c).

BC experiences two continuous weight loss steps in the range of 290–330 °C and 330–432 °C, respectively, accompanied with two endothermic peaks at about 321 and 388 °C in the DSC curve (Fig. S4a). The thermal degradation of BC was ascribed to dehydration, depolymerization, and decomposition of glycosyl units followed by the formation of a charred residue.[5, 6] Unlike pristine BC, BC/$TiO_2$ hybrid shows threestep weight-losses. The slight weight-loss before 170 ºC is ascribed to the loss of adsorbed and bonded water. The biggest and fastest weight loss that occurred in the range of 251–297 ºC with an endothermic peak at about 294 ºC is due to the thermal degradation of BC fibers. The last weight loss in 306–421 ºC range with an endothermic peak at about 381 ºC is the thermal degradation of BC fibers. Note that the decomposition temperature of BC/$TiO_2$ hybrid has shifted from about 290 °C to about 251 °C (Fig. S4b), suggesting earlier thermal decomposition of BC in the presence of $TiO_2$ coating, which is similar to the promotion of gold and $TiO_2$ nanoparticles on cellulose because of their catalytic effects.[7, 8] For $TiO_2$ nanotubes, the weight loss up to 800 ºC is only about 9% (Fig. S4c), indicating good thermal stability of $TiO_2$ nanotubes.

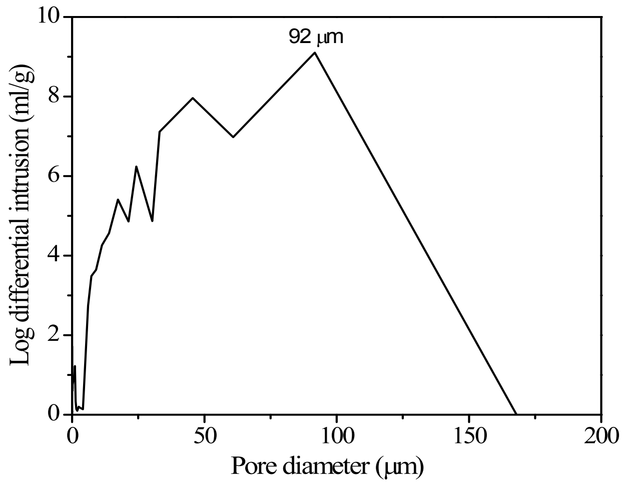


**Fig. S5** Pore size distribution of $TiO_2$ nanotube scaffold measured by mercury intrusion porosimetry.

## References


1. Y. Z. Wan, Y. Huang, C. D. Yuan, S. Raman, Y. Zhu, H. J. Jiang, F. He and C. Gao, *Mater. Sci. Engin. C*, 2007, **27**, 855-864.
2. C. Tokoh, K. Takabe, M. Fujita and H. Saiki, *Cellulose*, 1998, **5**, 249-261.
3. H. Luo, G. Xiong, Z. Yang, S. R. Raman, H. Si and Y. Wan, *RSC Adv.*, 2014, **4**, 14369-14372.
4. J.-P. Hsu and A. Nacu, *Langmuir*, 2003, **19**, 4448-4454.
5. H. S. Barud, A. M. de Araújo Júnior, D. B. Santos, R. de Assunção, C. S. Meireles, D. A. Cerqueira, G. Rodrigues Filho, C. A. Ribeiro, Y. Messaddeq and S. J. L. Ribeiro, *Thermochim. Acta*, 2008, **471**, 61-69.
6. M. Ul-Islam, T. Khan and J. K. Park, *Carbohydr. Polym.*, 2012, **89**, 1189-1197.
7. J. Cai, S. Kimura, M. Wada and S. Kuga, *Biomacromolecules*, 2009, **10**, 87-94.
8. J. Zeng, S. Liu, J. Cai and L. Zhang, *J. Phys. Chem. C*, 2010, **114**, 7806-7811.